Journal of Zhejiang University-SCIENCE A (Applied Physics & Engineering)
ISSN 1673-565X (Print); ISSN 1862-1775 (Online)
www.zju.edu.cn/jzus; www.springerlink.com
E-mail: jzus@zju.edu.cn

Cutting force and its frequency spectrum characteristics in high speed milling of titanium alloy with a polycrystalline diamond tool*

Peng LIU†, Jiu-hua XU, Yu-can FU

(*College of Mechanical and Electrical Engineering, Nanjing University of Aeronautics and Astronautics, Nanjing 210016, China*)

†E-mail: lpace@163.com

Received Sept. 17, 2010; Revision accepted Nov. 15, 2010; Crosschecked Dec. 10, 2010

Abstract: In this paper, a series of experiments were performed by high speed milling of Ti-6.5Al-2Zr-1Mo-1V (TA15) by use of polycrystalline diamond (PCD) tools. The characteristics of high speed machining (HSM) dynamic milling forces were investigated. The effects of the parameters of the process, i.e., cutting speed, feed per tooth, and depth of axial cut, on cutting forces were studied. The cutting force signals under different cutting speed conditions and different cutting tool wear stages were analyzed by frequency spectrum analysis. The trend and frequency domain aspects of the dynamic forces were evaluated and discussed. The results indicate that a characteristic frequency in cutting force power spectrum does in fact exist. The amplitudes increase with the increase of cutting speed and tool wear level, which could be applied to the monitoring of the cutting process.

Key words: Cutting force, High speed milling, Polycrystalline diamond (PCD) tool, Frequency spectrum analysis, Titanium alloy
doi:10.1631/jzus.A1000408 **Document code:** A **CLC number:** TG506

1 Introduction

Titanium and its alloys are considered to be difficult-to-machine materials because of their low thermal conductivity, high chemical reactivity, and low modulus of elasticity. This is attributed to their inherently high strength property maintained at elevated temperature and also their tendency to form localized shear bands during machining. Apart from that, the thermal conductivity of the TA15 alloy (8.8 W/(m·K)) is very low (83% lower) when compared to that of AISI 1045 steel (50 W/(m·K)), and the modulus of elasticity of the TA15 alloy (123 GPa) is also very low (40% lower) when compared to that of AISI 1045 steel (200 GPa). The heat-affected zone is also very small as a result of the shorter chip-tool contact length (about one-third of the contact length for steel) (López de lacalle *et al.*, 2000; Zoya and Krishnamurthy, 2000; Nabhani, 2001). As a result, high cutting temperatures are generated during the machining of titanium alloys, and the hottest point is brought close to the cutting edge. In addition, titanium alloys are generally difficult to machine at cutting speeds over 30 m/min with high speed steel (HSS) tools, and over 60 m/min with cemented tungsten carbide (WC) tools, which results in a very low productivity (López de lacalle *et al.*, 2000). The performance of conventional tools is poor when machining TA15 materials. With the evolution of a number of new cutting tool materials, advanced tool materials, such as cubic boron nitride (CBN) and polycrystalline diamond (PCD), have significant potential for use in high speed milling. Some of the ultra-hard materials, such as PCD and CBN, have been used in the machining of titanium alloys (König and Neise, 1993; Bhaumik *et al.*, 1995; Kuljanic *et al.*, 1998). Though both PCD and CBN are currently very expensive, they are expected to be the most suitable tools for titanium, because of their high hardness, high thermal conductivity, and excellent wear resistance. Both PCD and CBN are highly reactive with titanium alloys, but the formation of a titanium

* Project (No. IRT0837) supported by the Program for Changjiang Scholars and Innovative Research Team in University of China

carbide layer would protect the tool in forming a barrier to further diffusion (Budak and Altintas, 1995; Ezugwu *et al.*, 2005; Wang *et al.*, 2005; Sun *et al.*, 2009).

Cutting force is one of the important physical variables that embody relevant process information in machining. Such information can be used to assist in understanding critical machine attributes, such as machinability, cutter wear or fracture, machine tool chatter, machining accuracy, and surface finish (Nurul Amin *et al.*, 2007; Fang and Wu, 2009; Kikuchi, 2009; Antonialli *et al.*, 2010). The aim of this paper is to examine the effects of the milling parameters on cutting forces, and investigate the effect of cutting speed and cutting tool wear on the frequency spectrum characteristics of cutting forces in high speed milling of TA15 with a PCD tool.

2 Experiment

All of the high speed milling experiments were conducted on a MICRON UCP710 (MICRON, Switzerland) machining center with a maximum power of 16 kW. The maximum table feed and maximum spindle speed on this machine were 20 m/min and 18 000 r/min, respectively. PCD inserts of nose radius 0.4 mm (SECO XOEX 090304FR PCD20) were used in a SECO high-velocity end milling cutter to machine the blocks. The cutter had a rake angle of 0° and a flank angle of 15°. Single insert fly cutting was carried out for all of the tests in this research. The physical properties and nominal chemical composition of the inserts are given in Table 1. The work material to be studied was Ti-6.5Al-2Zr-1Mo-1V titanium alloy, a near-alpha alloy. Its nominal composition (%, w/w) and mechanical properties are shown in Tables 2 and 3, respectively.

The cutting force components acting on one tooth of the milling cutter and milling type are shown in Fig. 1, where the table system of cutting forces is (Alauddin *et al.*, 1998): F_x is the instantaneous normal component (the projection of resultant force in x direction); F_y is the instantaneous feed component (the projection of resultant force in y direction); and F_z is the instantaneous vertical component (the projection of resultant force in z direction).

The table system of cutting forces is stationary and does not depend on the kinematics of the cutting. The cutter system of cutting forces is: F_t is the instantaneous tangential component (the force passing

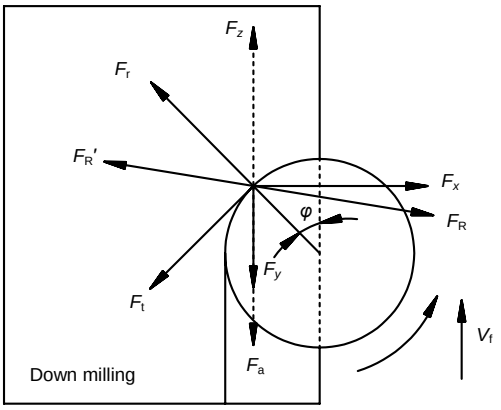

Fig. 1 Cutting force components acting on one tooth of a milling cutter (Alauddin *et al.*, 1998)

F_R: instantaneous resultant cutting force (table system) acting on the workpiece; F_R': instantaneous resultant cutting force (cutting system) acting on cutter; V_f: feed speed of the cutter

Table 2 Composition of TA15

Composition	Content (%, w/w)	Composition	Content (%, w/w)
Al	5.5–7.0	Mo	0.5–2.0
V	0.8–2.5	Ti	Balance
Zr	1.5–2.5		

Table 1 Properties of PCD insert

Chemical composition	Knoop hardness (GPa)	Density (g/cm^3)	Thermal conductivity at 20 °C (W/(m·K))	Average grain size (μm)
Diamond+Co-residue	50	4.12	540	10

Table 3 Mechanical properties of wrought TA15

Tensile strength (MPa)	0.2% proof stress (MPa)	Elongation (%)	Modulus of elasticity (GPa)	Knoop hardness (kg/mm^2)
1040	855–950	7–10	123	330–360

through the tangent to the circle circumscribed on the contour of the cutter cross-section); F_r is the instantaneous radial component (perpendicular to the cutter axis and acting along the radius of the cutter or tip of the tooth); and F_a is the instantaneous axial component (the force passing through the axis of the cutter). The tangential, radial and axial components of the cutting force on the tool, F_t, F_r, and F_a, respectively, are functions of instantaneous angle (φ) of the feed direction:

$$F_t=F_y\sin\varphi-F_x\cos\varphi, \quad (1)$$

$$F_r=F_y\cos\varphi+F_x\sin\varphi, \quad (2)$$

$$F_a=F_z. \quad (3)$$

A Kistler (model 9265B) three-component dynamometer was mounted between the workpiece and the machine table to measure cutting forces during machining. The force signals were acquired by a computer through a data acquisition program at a sampling frequency of 10 kHz. To analyze the cutting forces of the high-speed machining process, cutting forces were acquired while machining with a PCD tool at a feed between 0.02 and 0.08 mm per tooth. Eight different cutting speeds ranging from 50 to 400 m/min, and eight separate depths of axial cut between 0.1 and 0.8 mm were used for this purpose. Fig. 2 shows the original signals of the milling forces with a cutting speed of 300 m/min, a feed per tooth of 0.05 mm, and a depth of cut of 0.5 mm. Milling process is interrupted. It is a cutting cycle from teeth of the cutter cutting into the workpiece to cutting out. In a cutting cycle, cutting force increases to the maximum firstly, and then decreases to the minimum. Between the two cutting cycles, there is no cutting tooth, so the cutting force is zero if vibration is ignored.

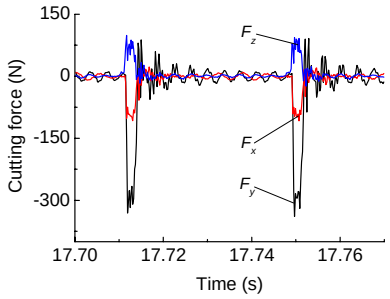

Fig. 2 Original signals of the milling forces with a cutting speed of 300 m/min, a feed per tooth of 0.05 mm, and a depth of cut of 0.5 mm

3 Results and discussion

3.1 Effects of milling parameters on cutting forces

Figs. 3–5 show the influences of the milling parameters on the three cutting components. Cutting force components in high speed milling of TA15 with a PCD tool is approximately between 50 and 300 N (Fig. 3), which is much smaller than a carbide tool (Xu *et al.*, 2004). Variation of average cutting force with the cutting speed is more complicated. As shown in Fig. 3, the cutting force increased initially with the cutting speed up to 100 m/min due to strain hardening. Then, a constant cutting force was followed within the cutting speed range 100–300 m/min, because the effect of strain hardening was equal to that of thermal softening. When the cutting speed exceeded 300 m/min, the cutting force decreased, which was attributed to thermal softening due to the increase of cutting temperature. Therefore, the temperature sensitivity of the workpiece predominates over the strain rate sensitivity within the cutting speed range. All of three-component cutting forces increased with the increase of the feed per tooth f (Fig. 4). It is because that as the feed per tooth increased, the area of shear plane increased in proportion due to increasing of undeformed chip thickness and constant of width of the uncut chip; thus, normal force on rake face increased. On the other hand, with increase of the feed per tooth, the average deformation coefficient of the chip was smaller, and the unit cutting force decreased. Thus, the increasing trend of main cutting force was reduced. Therefore, the cutting force would increase by about 70%–80% with the doubling of the feed per tooth. All of three-component cutting forces increased by the increase of the depth of cut a_p (Fig. 5). As the depth of cut increased, the area of shear plane and the contact area between chip and rake face increased proportionally due to the increase of uncut chip width, and the deformation and friction in the primary and secondary deformation zones correspondingly. Therefore, it can be stated cutting force increases with the axial depth of cut proportionally.

3.2 Effects of cutting speed on frequency domain of cutting forces

Figs. 6–8 shows the frequency spectra of F_t and F_r in different cutting speeds under cutting condition of a_p=0.5 mm and f=0.05 mm. A variation of frequency spectra of F_t and F_r was common.

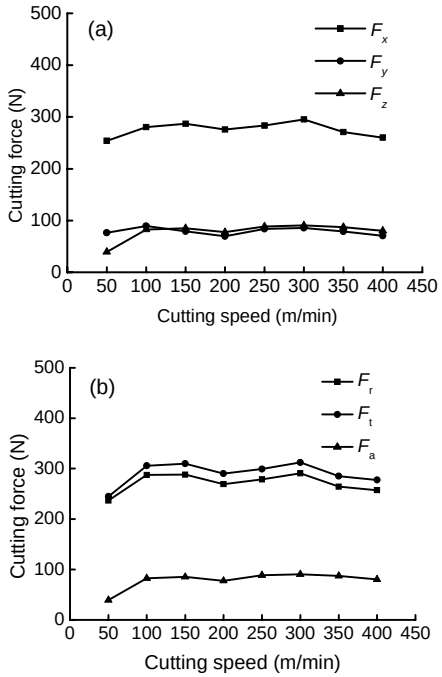

Fig. 3 Effects of cutting speed on the cutting force components with a depth of cut of 0.5 mm and a feed per tooth of 0.05 mm in the table system (a) and in the cutter system (b)

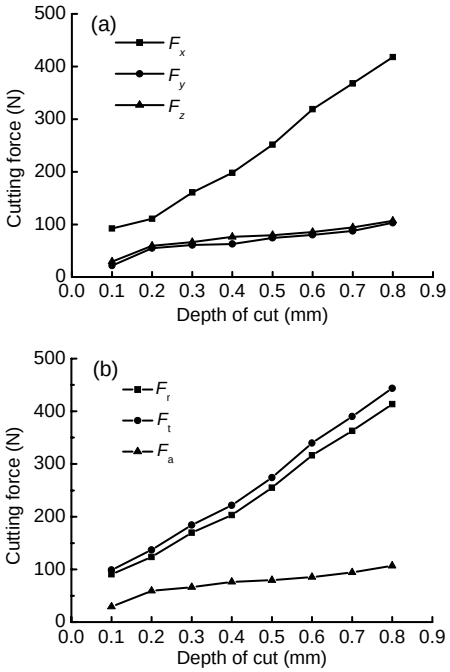

Fig. 5 Effects of depth of cut on the cutting force components with a cutting speed of 200 m/min and a feed per tooth of 0.05 mm in the table system (a) and in the cutter system (b)

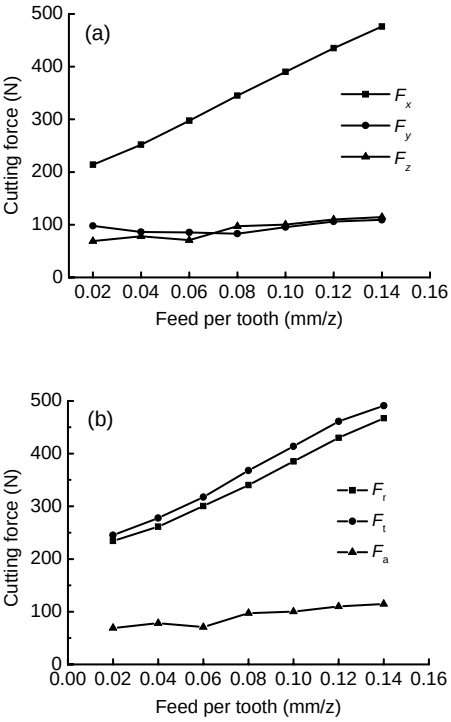

Fig. 4 Effects of feed per tooth on the cutting force components with a cutting speed of 200 m/min and a depth of cut of 0.5 mm in the table system (a) and in the cutter system (b)

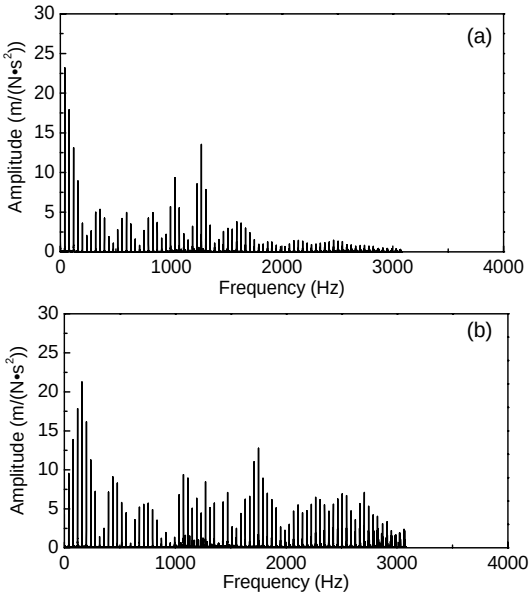

Fig. 6 Frequency spectra of the cutting force F_t (a) and F_r (b) under cutting speed of 150 m/min

Amplitude of cutting force signals was the maximum in the low-frequency stage, and decreased with an increase in frequency. The amplitude of cutting force signals increased again after a certain frequency and

the second peak formed. As shown in Fig. 6, the peak value of amplitude of cutting force signals appeared, when frequencies of F_t and F_r were 1.7 kHz, which were similar to the natural frequencies of the force sensor in the *x*-axis and *y*-axis directions used in the test. Therefore, the formation of the second peaks was the result of effects from the natural frequency of the force sensor on the cutting force signals. Therefore, to erase the effect of the measuring device, the cutting signal was filtered. The characteristics of frequency spectrum were studied in the low-frequency phase. The characteristic frequency was constant with the increase of cutting speed. However, the amplitude of cutting force signals under the characteristic frequency was changing with a variation of cutting speed. It increased as the cutting speed was increased. Figs. 9 and 10 show the effects of cutting speed on the amplitude of characteristic frequencies of F_t and F_r at about 1.2 kHz, respectively. The amplitude of the characteristic frequency increases with the increase of cutting speed. It can be used as an effective parameter to monitor the cutting process.

3.3 Effects of tool wear on frequency domain of cutting forces

Figs. 11–12 show the frequency spectra of F_t and F_r in different tool wear stages under the cutting condition of v=200 m/min, a_p=0.5 mm, and f=0.05 mm. The variation of frequency spectrum of F_t and F_r was quite common. The amplitude of the cutting force signals was the maximum in the low-frequency stage, and decreased with an increase in frequency. The amplitude of the cutting force signals increased again after a certain frequency and the second peak formed. Changes of characteristic frequency reflect the changes of the tool wear process

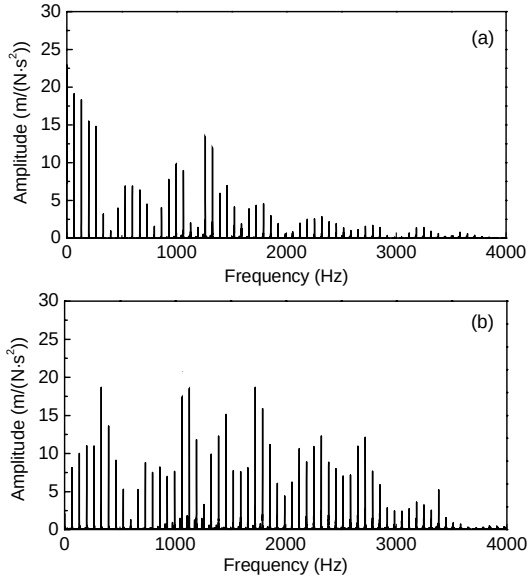

Fig. 7 Frequency spectra of the cutting force F_t (a) and F_r (b) under cutting speed of 250 m/min

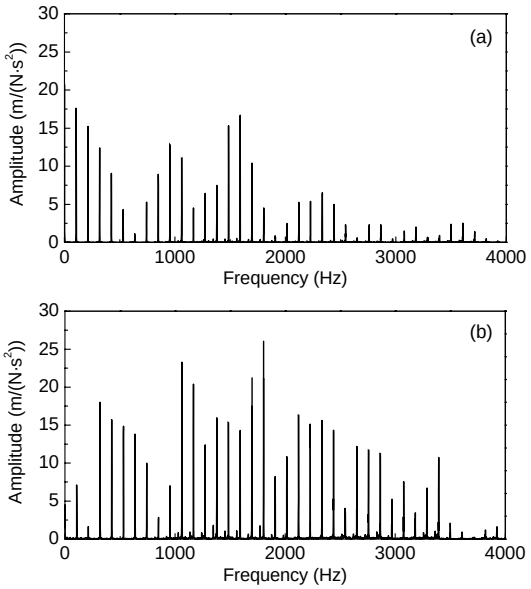

Fig. 8 Frequency spectra of the cutting force F_t (a) and F_r (b) under cutting speed of 400 m/min

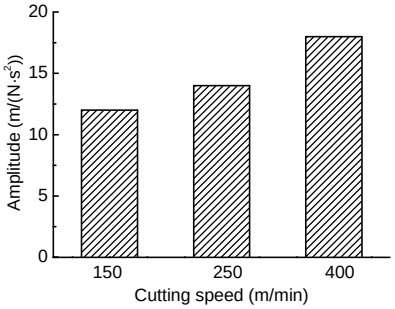

Fig. 9 Effects of cutting speed on the amplitude of characteristics frequency of F_t

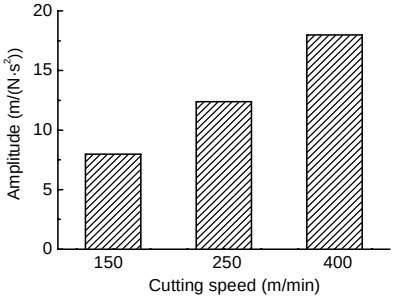

Fig. 10 Effects of cutting speed on the amplitude of characteristics frequency of F_r

due to constant cutting parameters. In different stages of tool wear, characteristic frequencies appeared in the low-frequency area, and its corresponding amplitude increased with the increase of tool wear.

Figs. 13 and 14 show the effects of tool wear on the amplitude of characteristic frequency of F_t and F_r at about 1.2 kHz, respectively. The amplitude of characteristic frequency increases with an increase in tool wear. Therefore, tool wear can be predicted according to the variation of corresponding amplitude of characteristic frequency.

4 Conclusions

The cutting forces and its frequency spectrum characteristics in high speed milling of titanium alloy with a PCD tool were investigated. The following conclusions can be drawn:

1. The axial depth of cut and tooth feed in milling parameters have significant effects on the cutting forces in high speed milling of the close titanium alloy. Effects of the cutting speed on cutting forces were not obvious.

2. In certain conditions, there were several characteristic frequencies in the low-frequency domain of cutting force signals, in which the amplitude of cutting force signals was the maximum. Corresponding amplitude of characteristic frequency increased with the increasing cutting speed.

3. In the cutting force spectrum, there were also a group of characteristic frequencies whose frequency and spectrum values are closely related to tool wear. The value of the spectrum increased with the increasing tool wear. Therefore, tool wear can be predicted according to variation of corresponding amplitudes of the characteristic frequency.

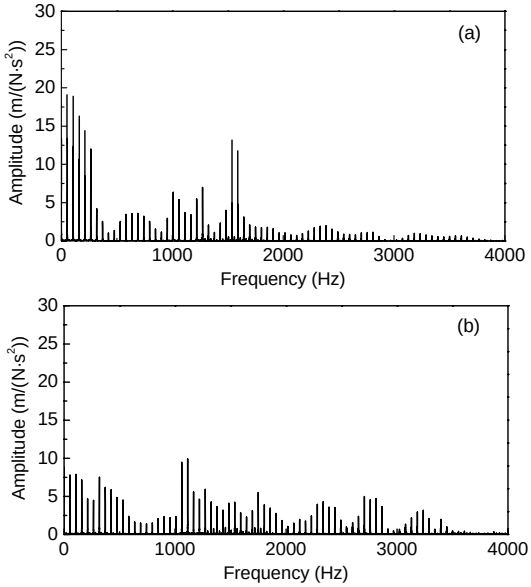

Fig. 11 Frequency spectra of the cutting force F_t (a) and F_r (b) under an average flank wear VB of 0.05 mm

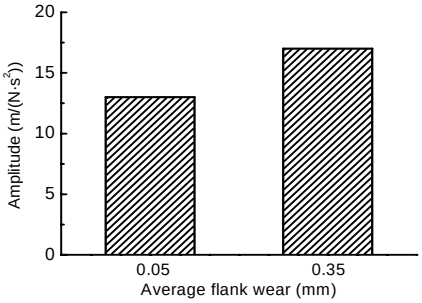

Fig. 13 Effects of tool wear on the amplitude of characteristic frequency of F_t

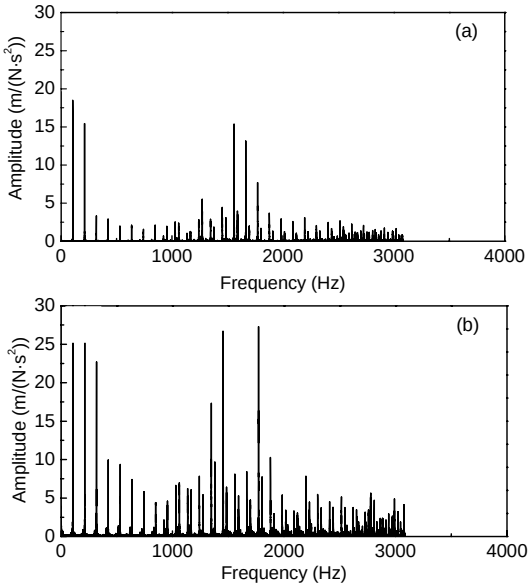

Fig. 12 Frequency spectrum of the cutting force F_t (a) and F_r (b) under an average flank wear VB of 0.35 mm

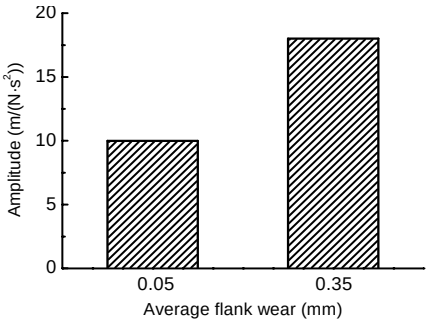

Fig. 14 Effects of tool wear on the amplitude of characteristic frequency of F_r

References

Alauddin, M., Mazid, M.A., El Baradi, M.A., Hashmi, M.S.J., 1998. Cutting forces in the end milling of Inconel 718. *Journal of Materials Processing Technology*, **77**(1-3): 153-159. [doi:10.1016/S0924-0136(97)00412-3]

Antonialli, A.I.S., Diniz, A.E., Pederiva, R., 2010. Vibration analysis of cutting force in titanium alloy milling. *International Journal of Machine Tools and Manufacture*, **50**(1):65-74. [doi:10.1016/j.ijmachtools.2009.09.006]

Bhaumik, S.K., Divakar, C., Singh, A.K., 1995. Machining Ti-6Al-4V alloy with a wBN-cBN composite tool. *Materials and Design*, **16**(4):221-226. [doi:10.1016/0261-3069(95)00044-5]

Budak, E., Altintas, Y., 1995. Modeling and avoidance of static form errors in peripheral milling of plates. *International Journal of Machine Tools and Manufacture*, **35**(3):459-476. [doi:10.1016/0890-6955(94)P2628-S]

Ezugwu, E.O., Da Silva, R.B., Bonney, J., Machado, A.R., 2005. Evaluation of the performance of CBN tools when turning Ti-6Al-4V alloy with high pressure coolant supplies. *International Journal of Machine Tools and Manufacture*, **45**(9):1009-1014. [doi:10.1016/j.ijmactools.2004.11.027]

Fang, N., Wu, Q., 2009. A comparative study of the cutting forces in high speed machining of Ti-6Al-4V and Inconel 718 with a round cutting edge tool. *Journal of Materials Processing Technology*, **209**(9):4385-4389. [doi:10.1016/j.jmatprotec.2008.10.013]

Kikuchi, M., 2009. The use of cutting temperature to evaluate the machinability of titanium alloys. *Acta Biomaterialia*, **5**(2):770-775. [doi:10.1016/j.actbio.2008.08.016]

König, W., Neises, N., 1993. Turning TiAl6V4 with PCD. *Industrial Diamond Review*, **53**(1):85-88.

Kuljanic, E., Fioretti, M., Beltrame, L., Miani, F., 1998. Milling titanium compressor blades with PCD cutter. *CIRP Annals-Manufacturing Technology*, **47**(1):61-64. [doi:10.1016/S0007-8506(07)62785-1]

López de lacalle, L.N., Pérez, J., Llorente, J.I., Sánchez, J.A., 2000. Advanced cutting conditions for the milling of aeronautical alloys. *Journal of Materials Processing Technology*, **100**(1-3):1-11. [doi:10.1016/S0924-0136(99)00372-6]

Nabhani, F., 2001. Machining of aerospace titanium alloys *Robotics and Computer-Integrated Manufacturing*, **17**(1-2):99-106. [doi:10.1016/S0736-5845(00)00042-9]

Nurul Amin, A.K.M., Ismail, A.F., Nor Khairusshima, M.K., 2007. Effectiveness of uncoated WC-Co and PCD inserts in end milling of titanium alloy—Ti-6Al-4V. *Journal of Materials Processing Technology*, **192-193**:147-158. [doi:10.1016/j.jmatprotec.2007.04.095]

Sun, S., Brandt, M., Dargusch, M.S., 2009. Characteristics of cutting forces and chip formation in machining of titanium alloys. *International Journal of Machine Tools and Manufacture*, **49**(7-8):561-568. [doi:10.1016/j.ijmachtools.2009.02.008]

Wang, Z.G., Rahman, M., Wong, Y.S., Li, X.P., 2005. A hybrid cutting force model for high-speed milling of titanium alloys. *CIRP Annals-Manufacturing Technology*, **54**(1):71-74. [doi:10.1016/S0007-8506(07)60052-3]

Xu, J.H., Ren, K.Q., Geng, G.S., 2004. Cutting forces in high-speed milling of a close alpha titanium alloy. *Key Engineering Materials*, **259-261**:451-455.

Zoya, Z.A., Krishnamurthy, R., 2000. The performance of CBN tools in the machining of titanium alloys. *Journal of Materials Processing Technology*, **100**(1-3):80-86. [doi:10.1016/S0924-0136(99)00464-1]